Fault Detection of Solar PV system using SVM and Thermal Image Processing

Karuppiah Natarajan*, B. Praveen Kumar **‡, Vankadara Sampath Kumar***

*Department of Electrical and Electronics Engineering, Vardhaman College of Engineering, Hyderabad (501 218), Telangana, India.

**Department of Electrical and Electronics Engineering, Bharat Institute of Engineering and Technology, Telangana, India

***Department of Electrical and Electronics Engineering, Bharat Institute of Engineering and Technology, Telangana, India

(natarajankaruppiah@gmail.com, praveenbala038@gmail.com, sampath.vankadara62@gmail.com)

‡ Praveen Kumar B, Bharat Institute of Engineering and Technology, Hyderabad, Telangana, India, Tel: +91 96296 32445, praveenbala038@gmail.com

Received: 10.04.2020 Accepted:07.05.2020

Abstract- Installation of photovoltaic plants across the globe increases, in the recent years, due to the energy demand across the world. Solar energy is free of cost, inexhaustible and a non-polluted source to the environment. The efficiency of any power plant depends on its fault free operation. Due to the occurrence of fault in PV system, the reliability and power output is reduced. In PV plants, the internal and external faults normally result in an increase in temperature which is easily sensed by different methods. In this paper, an algorithm based on thermal image processing, is proposed to extract the features of the PV cells in operation. These extracted features are then compared with the features of the healthy PV module using Support Vector Machine. SVM is a classifier tool which classifies whether the PV modules are defective or non-defective. An experimental set up is created and the performance of the algorithm is verified by testing it with faulty data sets which are obtained by creating different types of faults intentionally. The algorithm successfully identifies the defective PV module and its performance is validated experimentally.

Keywords PV faults, image processing, thermal images, texture information, maximum power.

1. Introduction

Nowadays the rapid growth in renewable energy has reduced the usage of fossil fuels. Since PV technology is an eco-friendly resource its usage has increased many folds. This reduces the greenhouse gas emissions to a great extent [1- 4]. Due to the climatic changes in the recent years, the PV panels experience stresses and thereby the performance is much affected. Normally the power output of a PV module depends on the irradiation (w/m^2) and the temperature (°C) [5-6]. The environmental changes have a direct impact on the amount of irradiance and temperature which results in the deterioration of PV module's efficiency [7-8]. In addition to this, partial shading, humidity, high temperature, bird droppings, dust accumulation etc., affects the efficiency of the PV system. Also, hotspots caused by the internal faults results in power loss of the PV system [9-13].

Researchers of today work to maximize the performance of the PV system thereby ensuring its reliable operation [14-16]. Depending on the characteristic curves of PV system, its state of operation is classified. A PV module gives its power output based on the irradiance and temperature level. The power output also depends on the maximum current, voltage and power of the module. Based on the manufacturer's data and the irradiance, temperature level the normal power output of the PV module is estimated [17-18]. This power output is termed as the normal operating state of the PV module. If the power output varies drastically from its expected normal output then the PV module is said to be faulty. Normally PV plant is an array of PV modules in which number of PV cells are connected in series and parallel depending on its desired power output. If the power output varies from the expected level, one or more PV cells could be faulty, depending on the severity of fault. Hence a fault monitoring and diagnostic system is to be developed for

the better operation of the PV plant [19-20]. The different types of possible faults on the PV system is listed in Table 1.

Table 1. Types of Faults

Sl. No	Fault Location	Types of Fault
1	On PV module	1. Encapsulation failure 2. Back sheet adhesion loss 3. Cells cracking 4. Broken interconnection 5. Shading & soiling 6. Hotspots 7. Module corrosion 8. Potential induced degradation 9. Light induced power degradation
2	Inverter Failure	1. Manufacturing / Designing failure 2. Control Problems 3. Electrical component failure
3	Other Failure Modes	1. Unbalance of the system 2. Junction box failure 3. By-pass diode failure 4. Mismatch fault 5. Ground Fault 6. Line-line fault 7. Arc Fault

Apart from the monitoring system it is necessary to have fault detection system to avoid the failure [21-22]. In general, major fault has been developed from several minor faults. Thus, the major fault is prevented by identification at the minor level [23-24]. In earlier literatures, the electrical data was used as a measure for identifying the fault [25-26]. Later the similar problems were resolved using soft computing techniques by considering it as an optimization problem. ANN based fault detection technique measures the MPP voltage and current from the MPPT controller and classifies the operating state as, normal state, degraded state, shaded state and the short circuit fault state. But this method was not successful in preventing major faults due to its limitations [27-28]. Another soft computing-based method is decision tree-based algorithm. In this method irradiation, current and voltage are the reference values and are used to train the algorithm and it flows like branches and leaves like the tree. Based on the number of trees and branches the type and level of fault was determined [29]. Mutually comparing algorithm, minimum covariance determinant estimator-based algorithm, analysis of variance-based algorithm are some other soft computing techniques used for determining fault in PV system [30]. Recent literature regarding partial shading, MPPT algorithms, Lab VIEW and reconfiguration techniques for solar panel applications and fault detection were analyzed [31-36].

Performance Ratio of the PV system is the ratio between the instantaneous values to the nominal value. Many researchers have developed fault monitoring and diagnostic system which do not take account of the instantaneous value of power output. Hence the severity of fault could not be estimated. A new kind of fault detection method has been discussed in this paper. This approach is based on the thermal image processing with a machine learning tool. The thermal camera is used for taking samples from the PV system and thereby extracting features of it. Using the machine learning tool like SVM, the features are fed into it and by comparing it with the reference samples it is classified into two types as defective and non-defective.

2. Creation of Faults

Different types of faults that are intentionally created are cracks, hot spots due to shading and soiling. The nature of different types of faults, possibility of occurrence of faults and its effects are discussed. These faults are intentionally created on a 3*3 PV array as shown in Figure 1 and its behaviour is checked to identify the healthy and faulty PV cell.

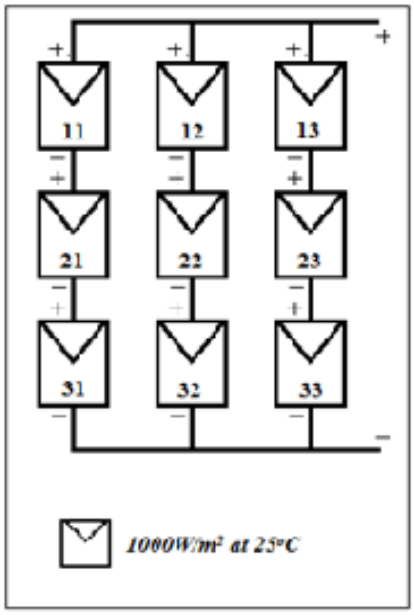

Fig. 1. Connection of PV cells in 3*3 array

2.1. Crack

Cracks on the PV panels are formed during transportation, severe climatic disturbances such as strong

winds, hail storms and improper handling of the panels during installation etc. The formation of cracks results in the decreased PV power output. Micro cracks are mainly due to the thermal stresses on the solar panel. During the production, these micro cracks occur on the surface of the panel during its lamination. Also, when materials like copper and silicon expands it creates micro cracks resulting in a higher resistance of the PV cell. Figure 2 shows the intentional cracks created on PV cells numbering 12, 23 and 31 in a 3*3 PV array due to thermal stress on the module.

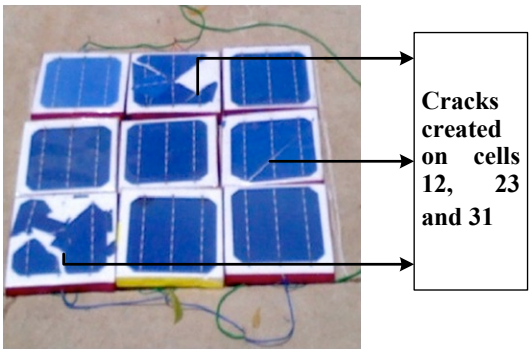

Fig. 2. Intentional cracks made on 3*3 PV array

2.2. Soiling

Soiling refers to the accumulation of soil, dust particles, etc. on the solar module. This soil accumulation restricts the amount of solar irradiance to pass into the module. This leads to the reduction of power output of the solar module. The factors affecting soiling and the power loss are climatic conditions, tilt angle of modules and type of liquid used for cleaning.

Climatic conditions: The dry condition with continuous flowing of wind would cause accumulation of soil and dust particles on the solar module and this process is called as cementing. This cemented dust particles are mostly irremovable which causes a fixed reduction of power output from the module and further damaging the module permanently.

Tilt angle of modules: The optimum tilt angle is the latitude of a particular location. Due to space constraints and to reduce the shadowing effect, sometimes the tilt angle is kept low from the actual. In such cases more dust accumulation occurs on the solar panel and decreases the power output.

Type of liquid used for cleaning: This factor has a direct impact on the efficiency of solar module. The chemical composition of the liquid used for cleaning contributes to this cause. Generally small droplets would be left over on the panel after the cleaning process. When this left-over cleaning liquid is evaporated, the chemical substance left over accumulates on the surface of the panel and restricts the amount of sunlight falling on it. Figure 3 shows the intentional soiling fault created on PV cells numbering 11 and 31 in a 3*3 PV array.

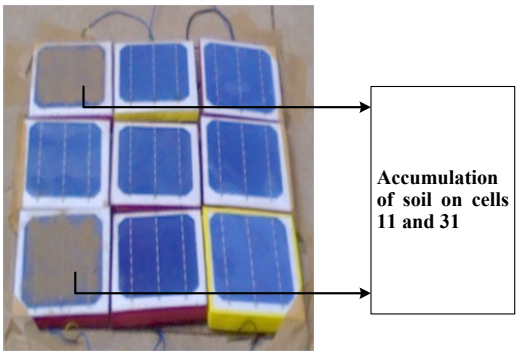

Fig. 3. Intentional accumulation of soil on 3*3 PV array

2.3. Hotspots due to shading

Hot spots appear when a solar cell within a module generates less current than the string current of the module. Hot spots are due to shading of trees and internal module failures. This results in temperature difference which affects the output current. Figure 4 shows the intentional hot spots created on PV cells numbering 13, 21, 32 and 33 in a 3*3 PV array. Full shading is shown in PV cells numbering 13 and 21. Similarly partial shading is shown in PV cells numbering 32 and 33.

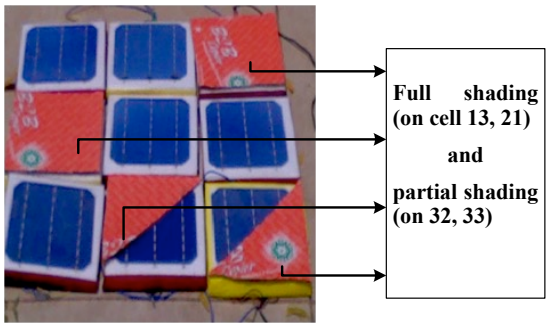

Fig. 4. Intentional Hot spot on 3*3 PV array

2.4. Combined Faults

Faults due to soiling, hot spots, internal failures and cracks are combined on the PV array and its behaviour is identified using thermal imaging and the faulty and non-faulty samples are classified using SVM. Figure 5 shows the combined faults created on PV cells numbering 13, 23, 32 and 31 in a 3*3 PV array. Crack is shown in PV cells numbering 13, 23 and 32. Similarly soiling is shown in PV cells numbering 31. Figure 6 shows the combined faults created on PV cells numbering 13, 21 and 33 in a 3*3 PV array. Shading is shown in PV cells numbering 13 and 21. Similarly soiling is shown in PV cells numbering 33.

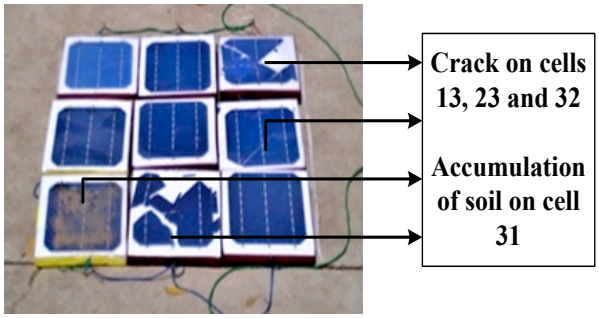

Fig. 5. Combined Faults on 3*3 PV array (cracks, soiling)

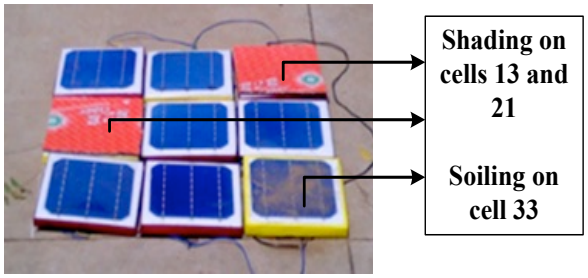

Fig. 6. Combined Faults on 3*3 PV array (shading, soiling)

3. Methodology

The fault detection in the PV array is done using a thermal imaging camera and Support Vector Machine. The flowchart of the proposed algorithm is shown in Figure 7.

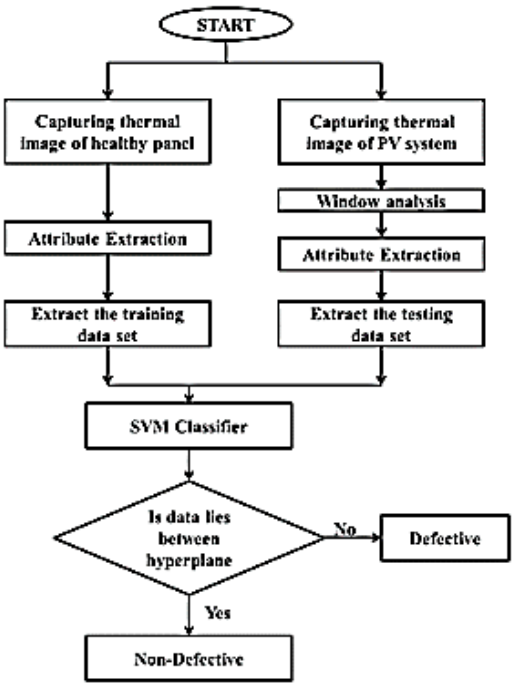

Fig. 7. Flow chart of proposed algorithm

The image of a healthy PV panel is captured using a thermal imaging camera. Then its features are extracted using MATLAB image processing code. The extracted features are then trained and considered as standard data set for Support Vector Machine. Now intentionally different faults are introduced on the surface of PV panel. Then the combined faulty PV panel's image is captured using a thermal imaging camera. Its features are again extracted using MATLAB code and trained and then compared with the standard data set using SVM. If the data lies between the hyperplane in SVM then the PV panel is said to be in healthy state. Otherwise it is considered as faulty.

Contrast is the information about the local variation in the GLCM expressed as per equation (1)

$$Contrast = \sum_{i,j=0}^{n-1}(i-j)^2 X\, m_{ij} \quad (1)$$

Correlation is the measure of the joint probability occurrence of the specific pixel pairs as per equation (2)

$$Correlation = \sum_{i,j=0}^{n-1} {(i-\mu)X(j-\mu)Xm_{ij}}/{1+\sigma^2} \quad (2)$$

Energy is the texture information which provides the sum of squared elements in the GLCM. It also known as the uniformity or the angular moment as shown in equation (3)

$$Energy = (\sum_{i,j=0}^{n-1} m_{ij}^2)^{1/2} \quad (3)$$

Homogeneity is the measure of the closeness of the distributed elements in the GLCM to the GLCM diagonal as in equation (4)

$$Homogeneity = \sum_{i,j=0}^{n=1} {m_{ij}}/{1+|i-j|^2} \quad (4)$$

Where i, j are the rows and columns of the matrix

m_{ij} is the pixel location

n-1 is the total no of rows and columns

μ is the mean

σ is the variance

The texture information of the healthy panels at standard test condition (STC) is shown in Table 2.

Table 2. Textural Information of Healthy PV cell

Texture	Value
Contrast	0.1282
Correlation	0.7223
Energy	0.5407
Homogeneity	0.9399
Entropy	5.3294
Standard Deviation	11.8869
Mean	88.8742

For classifying the PV cell using the derived texture information, SVM based classifier is used. SVM is one of the standard and simplest machine learning algorithms used for the classification problems as compared to other soft computing techniques like neural networks.

3.1 Data Raw Input

The texture information of the thermal image is treated as the raw input to the SVM classier. Based on this textural data, the SVM classifies the PV cell into two classifications as defective and non-defective. The steps followed in classifying the samples as healthy and faulty using SVM is shown in Figure 8.

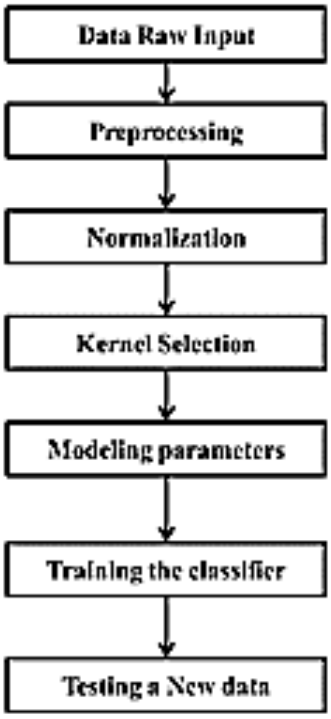

Fig. 8. Steps involved in SVM

3.2 Pre-processing

The SVM classifier will not recognize the raw inputs obtained from the feature extraction. Hence it is necessary to convert all the raw data into the numerical format which the SVM classifier can recognize.

3.3 Normalization

Data normalization is the important step to be carried out to execute the classification using SVM. The use of normalization process is to use the small sized attributes in the classification without neglecting them. If X is the pre-processed data, then the data normalization can be performed using the normalization function in the equation (5).

$$X' = a + \frac{(X - X_{min})(b-a)}{X_{max} - X_{min}} \quad (5)$$

Where, X' is the Normalized data value, Xmax and Xmin are the maximum and minimum data value in the domain of X, a is the maximum value in the output range, b is the minimum value in the output range.

3.4 Kernel selection

The SVM tries to obtain a separating hyper plane with the maximal margin for the classification. It chose a kernel function for obtaining the hyper plane. The kernel function selection is shown in the equation (6).

$$K(x_i, x_j) = \varphi(x_i)^T \varphi(x_j) \quad (6)$$

SVM uses four kinds of kernels based on the problem definition. In this problem, the classification is a linear problem. For this the SVM uses the linear kernel function for classifying the defected and non-defected PV cell.

3.5 Modeling Parameters

For the Linear kernel, C is the required parameter need to select before the kernel function. C parameter determines the influence of the misclassification on the objective function. It tells the optimization to avoid the misclassifying of each training data. The accuracy of the SVM classifier directly depends on this parameter. LIBSVM (Library for Support Vector Machine) is used for optimizing the C parameter by the cross validation.

For the large values of C, the optimization chose a small margin hyper plane and gives better accuracy, For the small value of C, the optimizer chooses a large margin, and it misclassifies many points. The sequences used here is C = [10-5, 10-4,……..,104,105]. This classifier is trained on the basis of pair that gives the better cross-validation accuracy.

3.6 Training the Classifier

After the selection of kernel and the model parameter, the SVM classifier is trained on the training data set. The textural information of the healthy PV panel is selected as the trained data set. It is trained to classify the defected PV cell.

3.7 Testing a New Data

The SVM classifier is capable of classifying the test data, when it was trained once. The textural information of the unknown PV cell is trained with the SVM classifier to characterize it as defective or non-defective.

The following steps are involved in the fault classification algorithm,

Step-1: Obtaining trained data sets from the healthy PV panel.

Step-2: Capturing thermal image of PV cell using FLIR T420bx.

Step-3: Window analysis using MATLAB tool for obtaining attribute

Step-4: Finding contrast, Correlation, energy, homogeneity, entropy, mean and standard deviation for the thermal image.

Step-5: Formulating the test data set.

Step-6: SVM classifier for obtaining fault level

Step-7: Non-defective cell satisfies the following condition

Hyper plane 1 ≤ testing data set ≥ Hyperplane 2

Step-8: Else it is a defective cell.

4. Results and Discussion

Before implementing the methodology to a higher end PV plant, the same is implemented with a lower order PV array. It is a 3*3 array of solar cell with series-parallel connections. Faults are intentionally created at various cells and thermal images of different cells are taken using thermal camera (FLIR E8). The features of the images such as standard deviation, mean, median etc. are examined using MATLAB code. Features are trained and tested in SVM and classified. Figure 9 shows a normal image of lower order PV system with 3*3 array of cells. Figure 10 shows the thermal images of 3*3 PV array with cracks alone, Figure 11 shows the thermal images of 3*3 PV array with soil accumulation alone, Figure 12 shows the thermal images of 3*3 PV array with full and partial shading and Figure 13 shows the thermal images of 3*3 PV array with combined faults.

Fig. 9. 3*3 PV Array Block diagram with faults

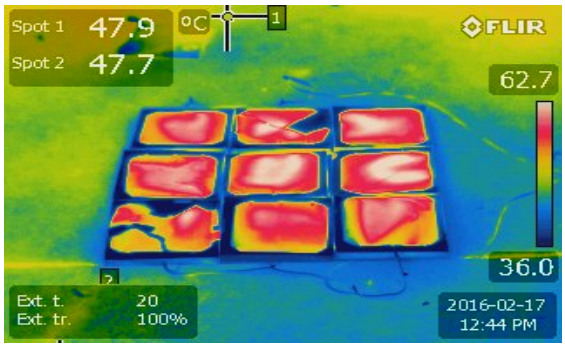

Fig. 10. Thermal image of 3*3 PV array with cracks

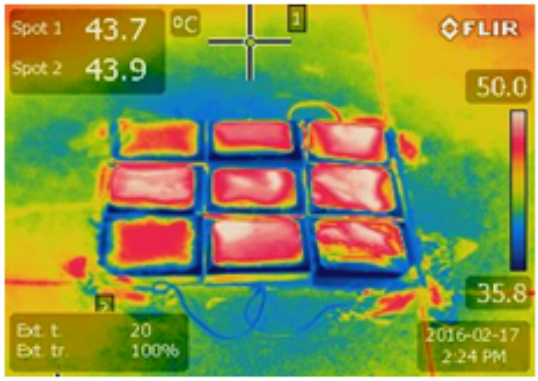

Fig. 11. Thermal image of 3*3 PV array with soil accumulation

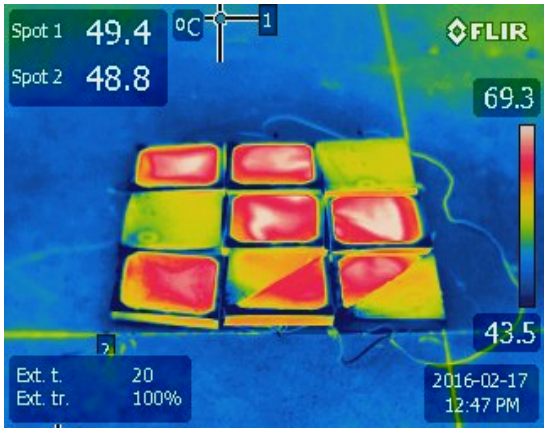

Fig. 12. Thermal imaging of 3*3 PV with full and partial shading

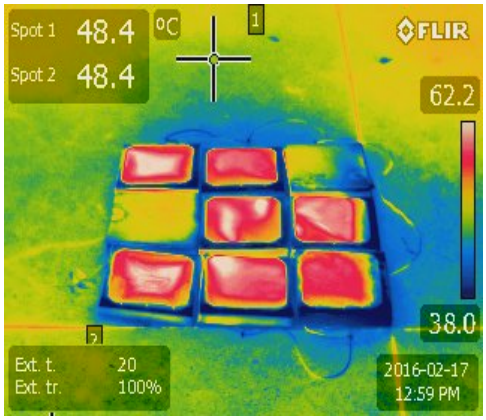

Fig. 13. Thermal imaging of 3*3 PV with combined fault

Training data were created for the solar PV array by considering the texture information like Entropy, mean, standard deviation (STD), Energy, Homogeneity, Correlation, and Contrast. For getting the texture information, the solar PV array is divided into individual panels and then each panel is split into four quadrants. Texture information is extracted from each quadrant of each cell. Accuracy depends on the number of splitting in a module. Similarly, testing data were also be collected and fed to the classifier for testing. Table 3 shows the training sample data of cell 11 and 21 during combined fault.

Table 3. Training data of Cell 11 and Cell 21

Texture	**Cell 11**				**Classifier output**
	Quadrant 1	**Quadrant 2**	**Quadrant 3**	**Quadrant 4**	
Standard Deviation	7.411	8.4247	6.7671	3.8588	**No Fault on 11**
Mean	29.56	58.92	39.28	36.16	**No Fault on 11**
Entropy	5.56	5.92	5.28	5.16	**No Fault on 11**
	Cell 21				
	Quadrant 1	**Quadrant 2**	**Quadrant 3**	**Quadrant 4**	
Standard Deviation	37.1489	10.6126	22.0599	2.5179	**Fault on 21**
Mean	143.72	206.72	219.08	215.44	**Fault on 21**
Entropy	143.72	206.72	219.08	215.44	**Fault on 21**

A 5 kWp PV plant is installed in 9° 42' 20.5956" N, 78° 5' 38.544" E, research location. This plant is being used for this research work and is shown in Figure 14. The 5 kWp PV plant is constructed with twenty numbers of monocrystalline PV panels of 250Wp each. FLIR T420bx model thermos graphic camera is being used in this work. Its resolution is 320*240 pixels. Each thermal image has 320*240 data in the matrix. Figure 15 shows the thermal image of the complete layout of PV system.

Fig. 14. Normal image of the 5kWp PV system

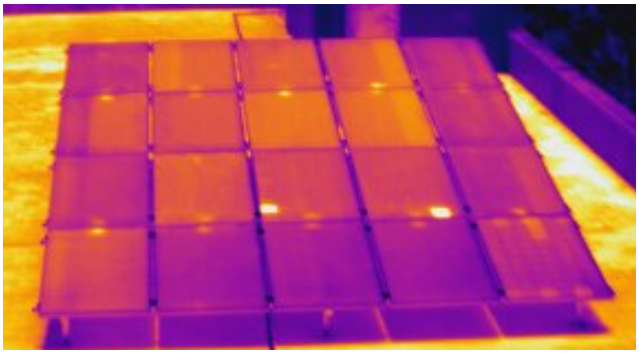

Fig. 15. Thermal image of the 5kWp PV system

Figure 16 shows the layout of PV array with intentionally created faults.

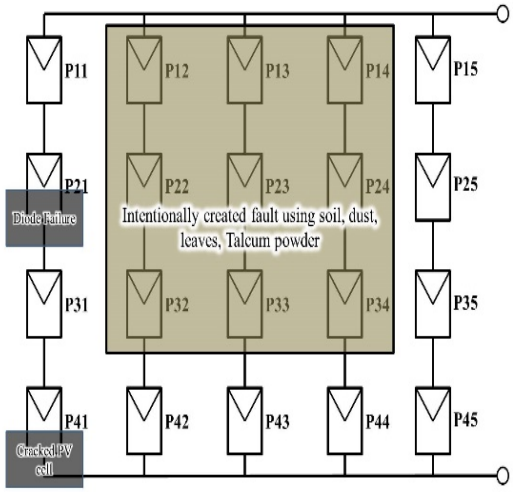

Fig. 16. PV Array Block diagram with fault location

To start or initialize the fault detection system, two images of a single PV cell is captured using a thermal image camera taken under the same environmental condition. The first thermal image is captured from the PV panel which generates rated power under specified environmental condition. This is used as the reference value or the training data set for the SVM classifier. The second thermal image captured is the entire PV system with the manual defects which are intentionally made. This image is used for generating the testing data set. The thermal and Gray scale images of healthy and defective PV cell is shown in Figure 17, 18, 19 and 20 respectively.

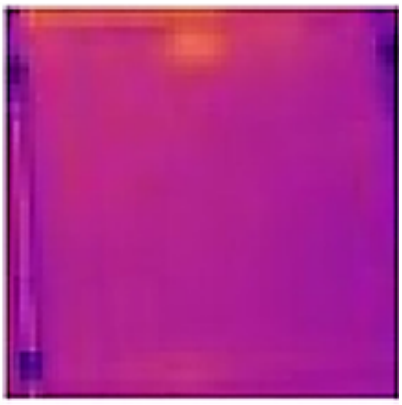

Fig. 17. Thermal image of a Non-Defective PV Cell

Fig. 18. Gray scale image of a Non-Defective PV Cell

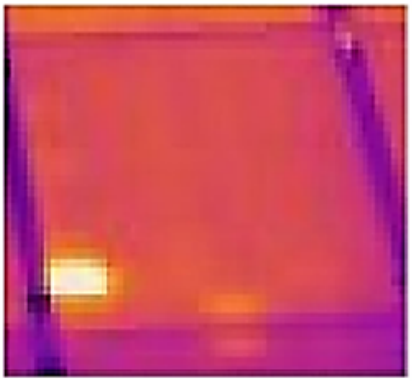

Fig. 19. Thermal image of a Defective PV Cell

The PV system is divided into twenty windows by using the MATLAB coding for obtaining the attributes of each panel. The attributes of the healthy panel is obtained by using the Gray Level Co-occurrence Matrix tool (GLCM). GLCM extracts the texture information of the image. The following required data are obtained from the textural information and is used for the fault classification.

Fig. 20. Gray scale image of a Defective PV Cell

SVM classifier is used to classifying all training vectors into two classifications. The training data set has derived from the textural information of healthy panel. The condition for validating the training data set has prepared with the bounding limits. The feature from the validation has selected to describe the best hyper parameter. The feature information from the individual window has trained with the hyper parameter of the SVM. This data are accumulating on the classifier region. The hyper parameters are the factor which forms a boundary between the two classifications. The data set that lies between the hyper parameter is classified under the non-defective classification and the remaining data sets are classified under the defective classification. The table shows the feature details of each window and the classification.

The defective classification is the output of this work. Two thermal images give the fault classification and it eliminates the need of electrical, environmental data analysis. It reduces the time period for fault detection. The faults in the PV system have intentionally created for the output verification. Soil, dust, leaves are spread over the some PV cells, some other have minor and major cracks, some PV cells are degraded due to the high temperature and one PV cell has diode failure. These are the well-known faults whose electrical characteristics has also verified for confirming the faulty state. The PV cells are named as P11, P12, P13, P14 and up to P45. Totally there are twenty panels constructed as 4*5 PV array. Table 4 shows the textural information and SVM classifier output.

Table 4. Textural Information and Classifier output for the test system shown in Fig. 14

Panel No	**Texture Information**							**Classifier Output**
	Contrast	Correlation	Energy	Homogeneity	Entropy	Mean	STD	
P11	0.1244	0.7222	0.5432	0.9012	5.3294	88.8742	11.8869	Non defective
P12	0.1735	0.8885	0.7865	1.1321	5.7921	92.5641	23.4897	**Defective**
P13	0.2221	0.8876	0.6543	1.3211	5.6890	94.5432	17.4897	**Defective**

P14	0.1987	0.9453	0.5476	1.4322	5.7249	93.1568	18.5674	**Defective**
P15	0.1132	0.7212	0.5211	0.8954	5.2894	89.5893	9.5891	Non defective
P21	0.2876	0.8798	0.8756	1.2365	5.5643	96.4689	17.3194	**Defective**
P22	0.4345	0.8787	0.7676	1.4322	5.1486	93.7513	22.3214	**Defective**
P23	0.3324	0.9132	0.8654	2.3211	5.5641	91.3125	19.1064	**Defective**
P24	0.2765	0.9767	0.7643	1.8653	5.8794	94.6857	19.7613	**Defective**
P25	0.1342	0.7321	0.5432	0.9986	5.2965	90.1963	13.4971	Non defective
P31	0.1238	0.7432	0.4567	0.9435	5.3156	89.8431	12.4681	Non defective
P32	0.3996	0.8786	0.6754	1.1239	5.8943	92.1854	19.4384	**Defective**
P33	0.4365	0.9786	0.7765	1.3242	5.8564	96.1289	18.3419	**Defective**
P34	0.3242	0.8987	0.8765	1.5421	5.5642	94.4965	21.1943	**Defective**
P35	0.1490	0.6997	0.5432	0.8675	5.1933	88.3467	14.3185	Non defective
P41	0.4326	0.8954	0.7656	1.2376	5.8797	92.8431	26.1354	**Defective**
P42	0.1476	0.7113	0.4599	0.9832	5.3216	87.4954	11.2734	Non defective
P43	0.1271	0.6987	0.5121	0.9213	5.2492	89.6579	9.2796	Non defective
P44	0.1995	0.7432	0.5421	0.9101	5.2945	90.7931	10.2349	Non defective
P45	0.1213	0.6543	0.4987	0.9012	5.3348	88.4688	11.1743	Non defective

5. Conclusions

In this paper, a simple image processing-based machine learning algorithm is performed for classifying the PV cell into two classifications. It is validated without considering the electrical parameters like current and power. It is inferred that, the cells which are in the defective classification gives the abnormal thermal output. The cells in the non-defective classification give the thermal output near to the expected values. In this work, the defects are intentionally created in the PV system for the analysis and the results obtained are 97% accurate with the comparison of test and training results. This fault classification technique is used in real time for the large PV system with very less computation time.

References

[1] S. Sharma, K. Kumar Jain, A. Sharma, "Solar Cells: In Research and Applications - A Review", Materials Sciences and Applications, Vol. 6, No. 12, pp. 1145-1155, December 2015.

[2] S. C. Bhatia, Advanced Renewable Energy Systems, Woodhead Publishing India Pvt. Ltd. 2014.

[3] T. S. Wurster and M. B. Schubert, "Mismatch loss in photovoltaic systems", Solar Energy, Vol. 105 pp. 505–511, July 2014.

[4] S. Gallardo-Saavedra, B. Karlsson, "Simulation, validation and analysis of shading effects on a PV system," Solar Energy, Vol. 170, pp. 828-839, August 2018.

[5] M. Ueshima, T. Babasaki, K. Yuasa and I. Omura, "Examination of Correction Method of Long-term Solar Radiation Forecasts of Numerical Weather Prediction", 8th International Conference on Renewable Energy Research and Applications (ICRERA), Brasov, Romania, pp. 113-117, 2019.

[6] M. R. Rashel, A. Albino, M. Tlemcani, T. C. F. Gonçalves and J. Rifath, "MATLAB Simulink modeling of photovoltaic cells for understanding shadow effect", IEEE International Conference on Renewable Energy Research and Applications (ICRERA), Birmingham, pp. 747-750, 2016.

[7] S. Osawa, T. Nakano, S. Matsumoto, N. Katayama, Y. Saka and H. Sato, "Fault diagnosis of photovoltaic modules using AC impedance spectroscopy", IEEE International Conference on Renewable Energy Research and Applications (ICRERA), Birmingham, pp. 210-215, 2016.

[8] B. Veerasamy, A. R. Thelkar, G. Ramu and T. Takeshita, "Efficient MPPT control for fast irradiation changes and partial shading conditions on PV systems", IEEE International Conference on Renewable Energy Research and Applications (ICRERA), Birmingham, pp. 358-363, 2016.

[9] M. Ünlü, S. Çamur, E. Beşer and B. Arifoğlu, "A new method for tracking the global maximum power point for grid-connected pv system under partially shaded conditions", IEEE International Conference on Renewable Energy Research and Applications (ICRERA), Birmingham, pp. 867-872, 2016.

[10] M. Dhimish, V. H., B. Mehrdadi, M. Dales, P. Mather, "PV output power enhancement using two mitigation techniques for hot spots and partially shaded solar cells", Electric Power Systems Research, Vol. 158, pp. 15-25, May 2018.

[11] R. Eke, T. R. Betts, R. Gottschalg, "Spectral irradiance effects on the outdoor performance of photovoltaic modules", Renewable and Sustainable Energy Reviews, Vol. 69, pp. 429-434, March 2017.

[12] A. Mohapatra, B. Nayak, P. Das, K. Barada Mohanty, "A review on MPPT techniques of PV system under partial shading condition," Renewable and Sustainable Energy Reviews, Vol. 80, pp. 854-867, December 2017.

[13] F. Belhachat, C. Larbes, "Comprehensive review on global maximum power point tracking techniques for PV systems subjected to partial shading conditions," Solar Energy, Vol. 183, pp. 476-500, May 2019.

[14] Chouder and S. Silvestre, "Automatic supervision and fault detection of PV systems based on power losses analysis", Energy Conversion and Management, Vol. 51, No. 10, pp. 1929–1937, 2010.

[15] M. Dhimish, V. Holmes and M. Dales, "Parallel fault detection algorithm for grid-connected photovoltaic plants", Renewable Energy, Vol. 113, pp. 94-111, 2017.

[16] K. Lappalainen and S. Valkealahti, "Effects of PV array layout, electrical configuration and geographic orientation on mismatch losses caused by moving clouds", IET Renewable Power Generation, Vol. 11, No. 12, pp. 1565–1575, 2017.

[17] S. Silvestre, M. Aires da Silva, A. Chouder, D. Guasch and E. Karatepe, "New procedure for fault detection in grid connected PV systems based on the evaluation of current and voltage indicators", Energy Conversion and Management, Vol. 86, pp. 241–249, October 2014.

[18] M. Dhimish, V. Holmes, B. Mehrdadi and M. Dales, "Simultaneous fault detection algorithm for grid-connected photovoltaic plants", Renewable Energy, Vol. 113, pp. 94-111, 2017.

[19] Mohammed Tadj, Khalil Benmouiza, Ali Cheknane and Santiago Silvestre, "Improving the performance of PV systems by faults detection using GISTEL approach", Energy Conversion and Management, Vol 80, pp. 298-304, 2014.

[20] Md. Kamal Hossain and Mohd. Hasan Ali., "Transient stability augmentation of PV/DFIG/SG-based hybrid power system by parallel-resonance bridge fault current limiter", Electric Power Systems Research, Vol. 130, pp. 89-102, January 2016.

[21] M. Dhimish, V. Holmes, B. Mehrdadi and M. Dales, "Diagnostic method for photovoltaic systems based on six layer detection algorithm", Electric Power Systems Research, Vol. 151, pp. 26–39, 2017.

[22] M. Bressan, Y. El Basri, A.G. Galeano and C. Alonso, "A shadow fault detection method based on the standard error analysis of I-V curves", Renewable Energy, Vol. 99, pp. 1181-1190, 2016.

[23] Siva Ramakrishna Madeti and S. N. Singh, "Online modular level fault detection algorithm for grid-tied and off-grid PV systems", Solar Energy, Vol. 157, pp. 349–364, 2017.

[24] W. Chine, A. Mellit, V. Lughi, A. Malek, G. Sulligoi and A. Massi Pavan, "A novel fault diagnosis technique for photovoltaic systems based on artificial neural networks", Renewable Energy, Vol. 90, pp. 501-512, 2016.

[25] H. Mekki, A. Mellit and H. Salhi, "Artificial neural network-based modelling and fault detection of partial shaded photovoltaic modules", Simulation Modelling Practice and Theory, Vol. 67, pp. 1–13, 2016.

[26] Dhimish M, Holmes V, Mehrdadi B, Dales M and Mather P, "Photovoltaic fault detection algorithm based on theoretical curves modelling and fuzzy classification system", Energy, Vol. 140, No. 1, pp. 276 – 290, December 2017.

[27] Y. Zhao, L. Yang, B. Lehman, J. de Palma, J. Mosesian and R. Lyons, "Decision tree-based fault detection and classification in solar photovoltaic arrays", 27th Annual IEEE Applied Power Electronics Conference and Exposition (APEC), Orlando, pp. 93-99, 2012.

[28] L. L. Jiang and D. L. Maskell, "Automatic fault detection and diagnosis for photovoltaic systems using combined artificial neural network and analytical based methods," International Joint Conference on Neural Networks (IJCNN), Killarney, pp. 1-8, 2015.

[29] D. Prince Winston, B. Praveen Kumar, S. Cynthia Christabel, J. Ali Chamkha, Ravishankar Sathyamurthy, "Maximum power extraction in solar renewable power system - a bypass diode scanning approach", Computers and Electrical Engineering, Vol. 70, pp. 122-136, 2018.

[30] B. Praveen Kumar, "Implementation of a switched PV technique for rooftop 2 kW solar PV to enhance power during unavoidable partial shading conditions", Journal of Power Electronics, Vol. 17, No. 6, pp. 1600-1610, 2017.

[31] B. Meenakshi Sundaram, B. V. Manikandan, B. Praveen Kumar, "Combination of Novel Converter Topology and Improved MPPT Algorithm for Harnessing Maximum Power from Grid Connected

Solar PV Systems," Journal of Electrical Engineering & Technology, Vol. 17, pp. 733 – 746.

[32] D. Prince Winston, S. Kumaravel, B. Praveen Kumar, S. Devakirubakaran, "Performance improvement of solar PV array topologies during various partial shading conditions", Solar Energy-Vol. 196, pp.228–242, 2019.

[33] K. Jai Ganesh, N. Karuppiah, S. Ravivarman, Md. Asif, "Performance study of MATLAB modelled PV panel and conventional PV interfaced with LabVIEW", International Journal of Engineering & Technology, Vol. 7, No. 2.17, pp. 70 – 73, 2018.

[34] A. Mohammedi, D. Rekioua, N. Mezzai, "Experimental study of a PV water pumping system", Journal of Electrical Systems, Vol. 9, No. 2, pp. 212-222, 2013.

[35] K. Tadjine, S. Aissou, N. E. Mebarki, D. Rekioua, P. Logerais, "Development of a Lab VIEW Interface to Maximize the Photovoltaic Power under Different Outdoor Conditions", Proceedings of International Conference on Renewable and Sustainable Energy (IRSEC), 2017.

[36] M. Ghazi Batarseh, M. Eddin Za'ter, "A MATLAB Based Comparative Study Between Single and Hybrid MPPT Techniques for Photovoltaic Systems", International Journal of Renewable Energy Research, Vol. 9, No. 4, pp. 2023 – 2039, December 2019.